

# LHC diphoton Higgs signal in the Higgs triplet model with $Y=0$

Lei Wang, Xiao-Fang Han

*Department of Physics, Yantai University, Yantai 264005, China*

## Abstract

We study the implications of the LHC diphoton Higgs signal on the Higgs triplet model with  $Y=0$ , which predicts two neutral CP-even Higgs bosons  $h$ ,  $H$  and a pair of charged Higgs  $H^\pm$ . We discuss three different scenarios: (i) the observed boson is the light Higgs boson  $h$ ; (ii) it is the heavy Higgs boson  $H$ ; (iii) the observed signal is from the almost degenerate  $h$  and  $H$ . We find that the Higgs diphoton rates in the first two scenarios can be enhanced compared to the SM value, which can fit the Higgs diphoton data at the LHC well. Meanwhile, another CP-even Higgs boson production rate can be suppressed enough not to be observed at the collider. For the third scenario, the Higgs diphoton rate is suppressed, which is disfavored by the experimental data. Also, we study the correlations between  $h \rightarrow Z\gamma$  and  $h \rightarrow \gamma\gamma$  and find that the two rates have the positive correlations for the three scenarios.

PACS numbers: 14.80.Ec, 12.60.Fr, 14.70.Bh

## I. INTRODUCTION

Recently, the CMS and ATLAS collaborations have announced the observation of a new boson around 125.5 GeV [1, 2]. This observation is corroborated by the Tevatron search results which showed a  $2.5\sigma$  excess in the range 115-135 GeV [3]. The diphoton rate is sizably higher than the SM expectation while the signal rates of  $ZZ^*$  and  $WW^*$  are consistent with the SM values. There are still large uncertainties on the  $Vb\bar{b}$  and  $\tau\bar{\tau}$  channels.

The recent Higgs data has been discussed in the SUSY models[4], little Higgs models [5] and the extensions of Higgs field models, such as the two-Higgs-doublet model [6], the Higgs triplet model (Y=2) [7], the models with septuplet [8] and color-octet scalar [9]. In this work, we will study the implications of the LHC diphoton Higgs signal on the Higgs triplet model with Y=0 [10], which predicts two neutral CP-even Higgs bosons  $h$ ,  $H$  and a pair of charged Higgs  $H^\pm$ . The model has the more simplest particle spectrum than the two-Higgs-doublet model and the Higgs triplet model (Y=2). We will discuss three different scenarios: (i) the observed boson is the light Higgs  $h$ , and the heavy Higgs  $H$  is not observed at the LHC; (ii) it is the heavy Higgs  $H$ , and the light Higgs  $h$  is not observed at the LEP; (iii) the observed signal is from the almost degenerate  $h$  and  $H$ . Besides, we will study the correlations between  $h \rightarrow Z\gamma$  and  $h \rightarrow \gamma\gamma$ . Since both of the rates are loop-induced by charged particles, they should be closely correlated. Any new physics effects manifested in the diphoton decay should also alter the  $Z\gamma$  decay [11, 12]

Our work is organized as follows. In Sec. II we recapitulate the Higgs triplet model with Y=0. In Sec. III we discuss the LHC diphoton Higgs signal and the correlations between  $h \rightarrow Z\gamma$  and  $h \rightarrow \gamma\gamma$ . Finally, we give our conclusion in Sec. IV.

## II. HIGGS TRIPLET MODEL WITH Y=0

In the Higgs triplet model with Y=0 (HTM0), a real  $SU(2)_L$  triplet scalar field  $\Sigma$  with  $Y = 0$  is added to the SM Lagrangian in addition to the doublet field  $\Phi$ . These fields can be written as

$$\Sigma = \frac{1}{2} \begin{pmatrix} \delta^0 & \sqrt{2}\delta^+ \\ \sqrt{2}\delta^- & -\delta^0 \end{pmatrix}, \quad \Phi = \begin{pmatrix} \phi^+ \\ \phi^0 \end{pmatrix}. \quad (1)$$

The renormalizable scalar potential can be written as [13]

$$V(\Phi, \Sigma) = -\mu^2 \Phi^\dagger \Phi + \lambda_0 (\Phi^\dagger \Phi)^2 - \frac{1}{2} M_\Sigma^2 F + \frac{b_4}{4} F^2 + a_1 \Phi^\dagger \Sigma \Phi + \frac{a_2}{2} \Phi^\dagger \Phi F, \quad (2)$$

where  $F \equiv (\delta^0)^2 + 2\delta^+ \delta^-$  and all the parameters are real. The Higgs doublet and triplet fields can acquire vacuum expectation values

$$\langle \Phi \rangle = \frac{1}{\sqrt{2}} \begin{pmatrix} 0 \\ v_d \end{pmatrix}, \quad \langle \Delta \rangle = \frac{1}{2} \begin{pmatrix} v_t & 0 \\ 0 & -v_t \end{pmatrix} \quad (3)$$

with  $v^2 = v_d^2 + 4v_t^2 \approx (246 \text{ GeV})^2$ .

After the spontaneous symmetry breaking, the Lagrangian of Eq. (2) predicts the four physical Higgs bosons, including two CP-even Higgs bosons  $h, H$  and a pair of charged Higgs  $H^\pm$ . These mass eigenstates are in general mixtures of the doublet and triplet fields. The mass matrixes of neutral and charged Higgs bosons are [13]

$$\mathcal{M}_0^2 = \begin{pmatrix} 2\lambda_0 v_d^2 & -a_1 v_d/2 + a_2 v_d v_t \\ -a_1 v_d/2 + a_2 v_d v_t & 2b_4 v_t^2 + \frac{a_1 v_d^2}{4v_t} \end{pmatrix} \equiv \begin{pmatrix} A & B \\ B & C \end{pmatrix}, \quad \mathcal{M}_\pm^2 = \begin{pmatrix} a_1 v_t & a_1 v_d/2 \\ a_1 v_d/2 & \frac{a_1 v_d^2}{4v_t} \end{pmatrix}. \quad (4)$$

The physical mass eigenstates and the unphysical electroweak eigenstates are related by rotations through two mixing angles  $\theta_0$  and  $\theta_\pm$ :

$$\begin{pmatrix} h \\ H \end{pmatrix} = \begin{pmatrix} \cos \theta_0 & \sin \theta_0 \\ -\sin \theta_0 & \cos \theta_0 \end{pmatrix} \begin{pmatrix} \phi^0 \\ \delta^0 \end{pmatrix}, \quad (5)$$

$$\begin{pmatrix} H^\pm \\ G^\pm \end{pmatrix} = \begin{pmatrix} -\sin \theta_\pm & \cos \theta_\pm \\ \cos \theta_\pm & \sin \theta_\pm \end{pmatrix} \begin{pmatrix} \phi^\pm \\ \delta^\pm \end{pmatrix}. \quad (6)$$

Where the Goldstone boson  $G^\pm$  is eaten by the gauge bosons.

Since the experimental value of the  $\rho$  parameter is near unity [14],  $4v_t^2/v_d^2$  is required to be much smaller than unity. In our calculation,  $v_t$  is taken as 1 GeV. The mixing angle  $\theta_\pm$  is proportional to  $\frac{v_t}{v_d}$ , therefore it is very small. The charged Higgs mass is given as

$$M_{H^\pm}^2 = a_1 v_t \left( 1 + \frac{v_d^2}{4v_t^2} \right). \quad (7)$$

The neutral mixing angle  $\theta_0$  is given as

$$c_0 \equiv \cos \theta_0 = \frac{1}{\sqrt{2}} \left( 1 - \frac{A - C}{\sqrt{(A - C)^2 + 4B^2}} \right)^{1/2},$$

$$s_0 \equiv \sin \theta_0 = -\frac{1}{\sqrt{2}} \frac{B}{|B|} \left( 1 + \frac{A - C}{\sqrt{(A - C)^2 + 4B^2}} \right)^{1/2}. \quad (8)$$

Where

$$c_0 > \frac{1}{\sqrt{2}} \text{ for } C > A, \quad c_0 < \frac{1}{\sqrt{2}} \text{ for } C < A, \quad c_0 \rightarrow \frac{1}{\sqrt{2}} \text{ for } C \rightarrow A. \quad (9)$$

The neutral Higgs boson masses are given as

$$\begin{aligned} m_h^2 &= \frac{1}{2} \left( A + C - \sqrt{(A - C)^2 + 4B^2} \right), \\ m_H^2 &= \frac{1}{2} \left( A + C + \sqrt{(A - C)^2 + 4B^2} \right). \end{aligned} \quad (10)$$

In our calculations, the involved Higgs couplings are listed as [13]

$$\begin{aligned} hf\bar{f} &: -i \frac{m_f}{v_d} c_0, & Hf\bar{f} &: i \frac{m_f}{v_d} s_0, \\ ZZh &: \frac{2im_Z^2}{v_d} c_0 g^{\mu\nu}, & ZZH &: -\frac{2im_Z^2}{v_d} s_0 g^{\mu\nu}, \\ W^+W^-h &: ig_2^2 \left( \frac{1}{2} v_d c_0 + 2v_t s_0 \right) g^{\mu\nu}, & W^+W^-H &: ig_2^2 \left( -\frac{1}{2} v_d s_0 + 2v_t c_0 \right) g^{\mu\nu}, \\ \gamma H^+H^- &: ie (p' - p)^\mu, & ZH^+H^- &: i \left( g_2 c_W - \frac{m_Z}{v_d} s_+^2 \right) (p' - p)^\mu, \\ H^+H^-h &: -i \left( a_1 c_+ s_+ c_0 - \frac{1}{2} a_1 s_+^2 s_0 + a_2 v_d c_+^2 c_0 + a_2 v_t s_+^2 s_0 + 2b_4 v_t c_+^2 s_0 + 2\lambda_0 v_d s_+^2 c_0 \right), \\ H^+H^-H &: -i \left( -a_1 c_+ s_+ s_0 - \frac{1}{2} a_1 s_+^2 c_0 - a_2 v_d c_+^2 s_0 + a_2 v_t s_+^2 c_0 + 2b_4 v_t c_+^2 c_0 - 2\lambda_0 v_d s_+^2 s_0 \right). \end{aligned} \quad (11)$$

Where  $s_+ = \sin \theta_+$  and  $c_+ = \cos \theta_+$ . All the momenta flow into the vertex.

### III. THE HIGGS DIPHOTON AND $Z\gamma$ RATES AT THE LHC

In our calculations, we take  $m_h$ ,  $m_H$ ,  $a_2$ ,  $b_4$  and  $v_d$ ,  $v_t$  as the input parameters, which can determine the values of  $\lambda_0$ ,  $a_1$ ,  $m_{H^\pm}$ . As mentioned above,  $v_t$  is taken as 1 GeV. The perturbativity can give the strong constraints on  $a_2$  and  $b_4$ ,

$$-2\sqrt{\pi} \leq a_2 \leq 2\sqrt{\pi}, \quad -2\sqrt{\pi} \leq b_4 \leq 2\sqrt{\pi}. \quad (12)$$

The electroweak  $T$  parameter can give the constraints on the splitting of  $m_H$  and  $m_{H^\pm}$ ,  $(m_H - m_{H^\pm})^2 < 0.96 m_W^2$  [13]. Since the coupling  $H^\pm \bar{f}_i f_j$  is sizably suppressed by  $s_+$ , the search experiments through the top quark decay hardly give the constraints on  $H^\pm$ . The experimental data at the LEP gives the lower bound of the charged Higgs mass,  $m_{H^\pm} > 79.3$  GeV [15].

We discuss three different scenarios: (I) the observed boson is the light Higgs  $h$ ,  $m_h = 125.5$  GeV and  $135 \text{ GeV} \leq m_H \leq 500 \text{ GeV}$ ; (II) it is the heavy Higgs  $H$ ,  $m_H = 125.5$  GeV and  $80 \text{ GeV} \leq m_h \leq 110 \text{ GeV}$ ; (III) the observed signal is from the almost degenerate  $h$  and  $H$ ,  $m_h \simeq m_H \simeq 125.5$  GeV.

As shown in the Eq. (11), the  $h$  couplings to  $f\bar{f}$  and  $WW$  are proportional to  $c_0$  while these couplings of  $H$  are proportional to  $s_0$ . Due to  $v_t \ll v_d$  and  $s_+ \rightarrow 0$ , the  $h$  couplings to  $WW$  and  $H^+H^-$  are sensitive to  $c_0$  while these couplings of  $H$  are sensitive to  $s_0$ . Therefore, the cross sections and the decay widths of  $h(H)$  normalized to SM values can be given as

$$\begin{aligned} \frac{\sigma(gg \rightarrow h(H))}{\sigma_{SM}(gg \rightarrow h(H))} &\simeq \frac{\sigma(pp \rightarrow jjh(H))}{\sigma_{SM}(pp \rightarrow jjh(H))} \\ &\simeq \frac{\sigma(pp \rightarrow Vh(H))}{\sigma_{SM}(pp \rightarrow Vh(H))} \simeq \frac{\sigma(pp \rightarrow h(H)t\bar{t})}{\sigma_{SM}(pp \rightarrow h(H)t\bar{t})} \simeq c_0^2(s_0^2), \\ \frac{\Gamma(h(H) \rightarrow f\bar{f})}{\Gamma_{SM}(h(H) \rightarrow f\bar{f})} &\simeq \frac{\Gamma(h(H) \rightarrow VV)}{\Gamma_{SM}(h(H) \rightarrow VV)} \simeq \frac{\Gamma(h(H) \rightarrow gg)}{\Gamma_{SM}(h(H) \rightarrow gg)} \simeq c_0^2(s_0^2), \end{aligned} \quad (13)$$

where  $V$  denotes  $W$ ,  $Z$ . Compared to SM, in addition to the modified  $ht\bar{t}$  and  $hWW$  couplings, the charged Higgs  $H^\pm$  will alter the decays  $h \rightarrow \gamma\gamma$  and  $h \rightarrow Z\gamma$  via the one-loop. The corresponding expressions are given in the Appendix A.

The Higgs boson  $\gamma\gamma$ ,  $ZZ^*$  and  $Z\gamma$  rates of HTM0 normalized to the SM values are respectively defined as

$$\begin{aligned} R_{h(H)}(\gamma\gamma) &= \frac{\sigma(pp \rightarrow h(H))}{\sigma_{SM}(pp \rightarrow h(H))} \frac{Br(h(H) \rightarrow \gamma\gamma)}{Br_{SM}(h(H) \rightarrow \gamma\gamma)} \\ &\simeq c_0^2(s_0^2) \frac{\Gamma(h(H) \rightarrow \gamma\gamma)}{c_0^2(s_0^2)\Gamma_{SM}(h(H))} \frac{\Gamma_{SM}(h(H))}{\Gamma_{SM}(h(H) \rightarrow \gamma\gamma)} \simeq \frac{\Gamma(h(H) \rightarrow \gamma\gamma)}{\Gamma_{SM}(h(H) \rightarrow \gamma\gamma)}, \\ R_{h(H)}(ZZ^*) &= \frac{\sigma(pp \rightarrow h(H))}{\sigma_{SM}(pp \rightarrow h(H))} \frac{Br(h(H) \rightarrow ZZ^*)}{Br_{SM}(h(H) \rightarrow ZZ^*)} \\ &\simeq c_0^2(s_0^2) \frac{c_0^2(s_0^2)\Gamma_{SM}(h(H) \rightarrow ZZ^*)}{c_0^2(s_0^2)\Gamma_{SM}(h(H))} \frac{\Gamma_{SM}(h(H))}{\Gamma_{SM}(h(H) \rightarrow ZZ^*)} \simeq c_0^2(s_0^2), \\ R_{h(H)}(Z\gamma) &= \frac{\sigma(pp \rightarrow h(H))}{\sigma_{SM}(pp \rightarrow h(H))} \frac{Br(h(H) \rightarrow Z\gamma)}{Br_{SM}(h(H) \rightarrow Z\gamma)} \\ &\simeq c_0^2(s_0^2) \frac{\Gamma(h(H) \rightarrow Z\gamma)}{c_0^2(s_0^2)\Gamma_{SM}(h(H))} \frac{\Gamma_{SM}(h(H))}{\Gamma_{SM}(h(H) \rightarrow Z\gamma)} \simeq \frac{\Gamma(h(H) \rightarrow Z\gamma)}{\Gamma_{SM}(h(H) \rightarrow Z\gamma)} \end{aligned} \quad (14)$$

Where  $\sigma(pp \rightarrow h(H))$  is the total cross section of Higgs boson. The analytic expressions in Eq. (13) and Eq. (14) may help us understand the Higgs production and decay well. In our numerical calculations, we take code Hdecay to consider the relevant higher order QCD and electroweak corrections [16].

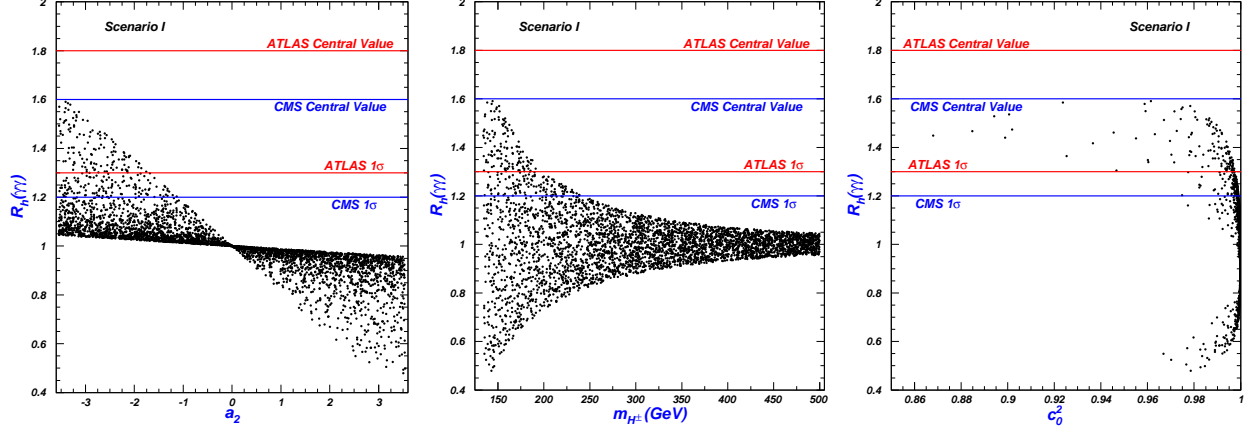


FIG. 1: The scatter plots of the parameter space projected on the planes of  $R_h(\gamma\gamma)$  versus  $a_2$ ,  $m_{H^\pm}$  and  $c_0^2$ , respectively.

The diphoton and  $ZZ^*$  are the cleanest channels for the Higgs boson. The CMS and ATLAS have presented the constraints [1, 2],

$$R_{\gamma\gamma} = 1.6 \pm 0.4, \quad R_{ZZ} = 0.8 \pm 0.3, \quad (\text{CMS})$$

$$R_{\gamma\gamma} = 1.8 \pm 0.5, \quad R_{ZZ} = 1.2 \pm 0.6. \quad (\text{ATLAS}) \quad (15)$$

The CMS collaboration has released their results of the measurement of  $Z\gamma$  and set an upper limit on the ratio  $R_{Z\gamma} < 10$  [17].

### A. Scenario I

For the scenario I, the light Higgs  $h$  is the observed boson. Since the observed  $ZZ^*$  rate is consistent with the SM value,  $c_0$  can not be too small. Also, it is important to make sure that the production rate of  $H$  is small enough not to be detected at the LHC. Thus, to obtain a large  $c_0$  and a small  $s_0$ , we require  $C > A$  (see Eq. (9)).

In Fig. 1, we plot  $R_h(\gamma\gamma)$  versus  $a_2$ ,  $m_{H^\pm}$  and  $c_0^2$ , respectively. The  $h$  coupling to  $H^+H^-$  is sensitive to the parameter  $a_2$ , which gives the additional contributions to the decay  $h \rightarrow \gamma\gamma$  via one-loop. The left panel shows that the  $H^\pm$  contributions to  $R_h(\gamma\gamma)$  can interfere constructively with  $W$  contributions for  $a_2 < 0$  and interfere destructively for  $a_2 > 0$ , leading  $R_h(\gamma\gamma) > 1$  and  $R_h(\gamma\gamma) < 1$ , respectively. The magnitude becomes sizable as the increasing of the absolute value of  $a_2$  and the decreasing of  $m_{H^\pm}$ . The ATLAS and CMS

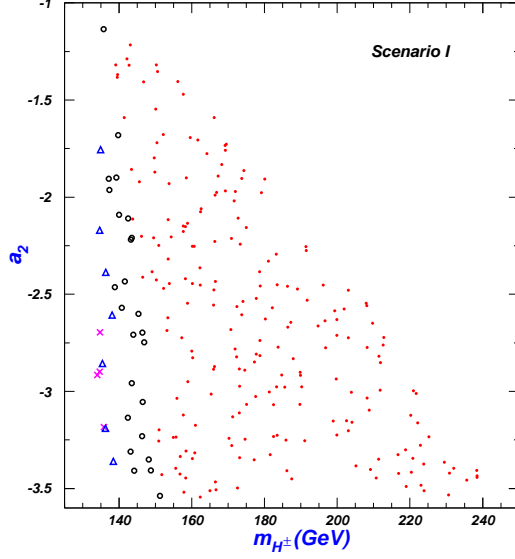


FIG. 2: The scatter plots for  $1.2 \leq R_h(\gamma\gamma) \leq 1.6$  projected on the plane of  $a_2$  versus  $m_{H^\pm}$ .  $0.86 < c_0^2 < 0.90$  for the crosses (pink),  $0.90 \leq c_0^2 < 0.95$  for the triangles (blue),  $0.95 \leq c_0^2 < 0.98$  for the circles (black), and  $0.98 \leq c_0^2 < 1.0$  for the bullets (red).

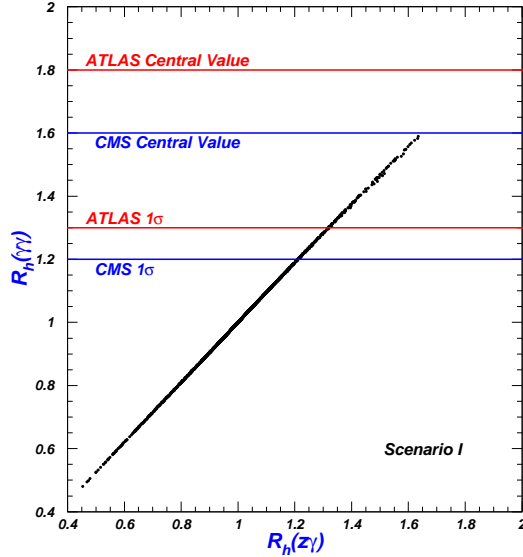


FIG. 3: The scatter plots of the parameter space projected on the plane of  $R_h(\gamma\gamma)$  versus  $R_h(Z\gamma)$ .

data favors  $-3.5 < a_2 < -1.0$  and  $m_{H^\pm} < 240$  GeV. The right panel shows that the scatter plots lie in the region of  $c_0^2 > 0.86$ , and the vast majority of them congregate the region of  $c_0^2 > 0.96$ . For such values of  $c_0$ , the  $ZZ^*$  rate of  $h$  is consistent with the experimental data. The corresponding  $s_0^2$  is smaller than 0.14, which will suppress the production rate of  $H$  at the LHC sizably, leading that  $H$  is not detected at the LHC.

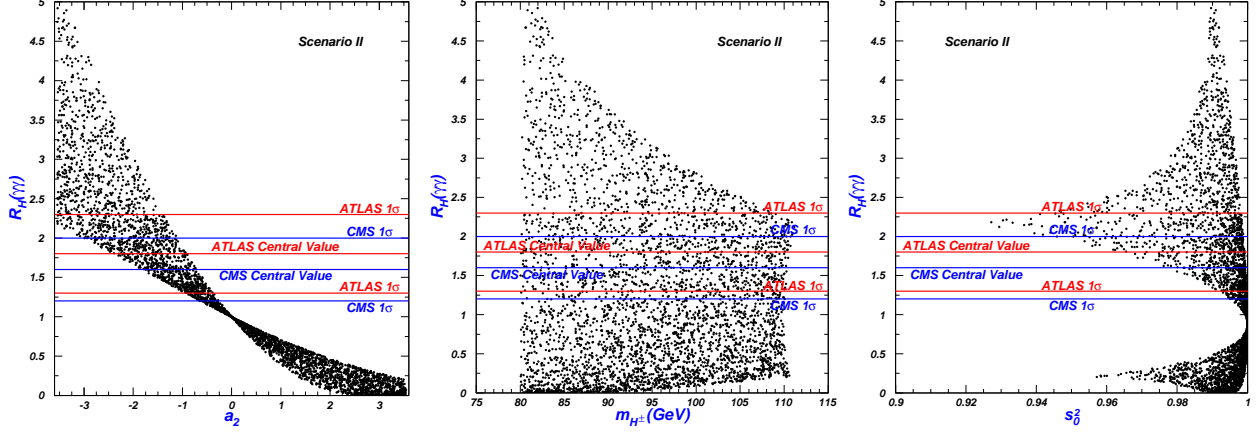


FIG. 4: Same as Fig. 1, but for  $R_H(\gamma\gamma)$ .

Fig. 2 shows  $a_2$  and  $m_{H^\pm}$  for which  $R_h(\gamma\gamma)$  is in the  $1\sigma$  range of the LHC data (1.2-1.6). The large  $m_{H^\pm}$  favors the large  $c_0^2$ , which leads that  $s_0^2$  is small and  $H$  is difficult to be detected at the LHC.

Fig. 3 shows  $R_h(\gamma\gamma)$  versus  $R_h(Z\gamma)$ . We find that the two rates are positively correlated, and the behavior of  $R_h(Z\gamma)$  is similar to that of  $R_h(\gamma\gamma)$ . Further, the prediction of  $R_h(Z\gamma)$  equals to that of  $R_h(\gamma\gamma)$  approximately.

## B. Scenario II

For the scenario II, the heavy Higgs  $H$  is the observed boson. The parameter  $s_0$  can not be very small to make the observed  $ZZ^*$  rate to be consistent with the experimental data. Besides, it is important to make sure that the production rate of  $h$  is small enough not to be detected at the LEP. Thus, we require  $C < A$  to obtain a large  $s_0$  and a small  $c_0$ , (see Eq. (9)).

In Fig. 4, we plot  $R_H(\gamma\gamma)$  versus  $a_2$ ,  $m_{H^\pm}$  and  $s_0^2$ , respectively. Similar to  $R_h(\gamma\gamma)$ ,  $R_H(\gamma\gamma)$  is also larger than 1.0 for  $a_2 < 0$  and smaller than 1.0 for  $a_2 > 0$ .  $R_H(\gamma\gamma)$  can reach 5.0 for  $a_2 \sim -3.5$  and  $m_{H^\pm} \sim 80$  GeV, which is much larger than  $R_h(\gamma\gamma)$  since  $m_{H^\pm}$  for the former is smaller than that for the latter. The right panel shows that the scatter plots lie in the region of  $s_0^2 > 0.92$ . For such values of  $s_0$ , the  $ZZ^*$  rate of  $H$  is consistent with the experimental data.

In Fig. 5, we plot  $a_2$  and  $m_{H^\pm}$  for which  $R_H(\gamma\gamma)$  is in the  $1\sigma$  range of the LHC data (1.2-2.3). The small  $m_{H^\pm}$  favors a large  $s_0^2$ , leading to a small  $c_0^2$ . For example,  $c_0^2$  is smaller



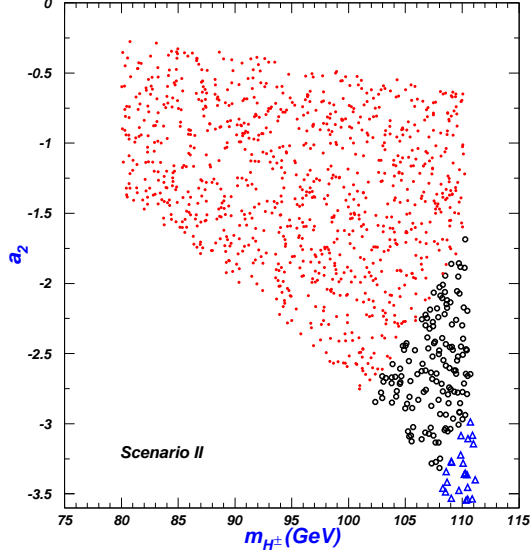


FIG. 5: The Scatter plots for  $1.2 \leq R_H(\gamma\gamma) \leq 2.3$  projected on the plane of  $a_2$  versus  $m_{H^\pm}$ .  $0.92 < s_0^2 < 0.95$  for the triangles (blue),  $0.95 \leq s_0^2 < 0.98$  for the circles (black), and  $0.98 \leq s_0^2 < 1.0$  for the bullets (red).

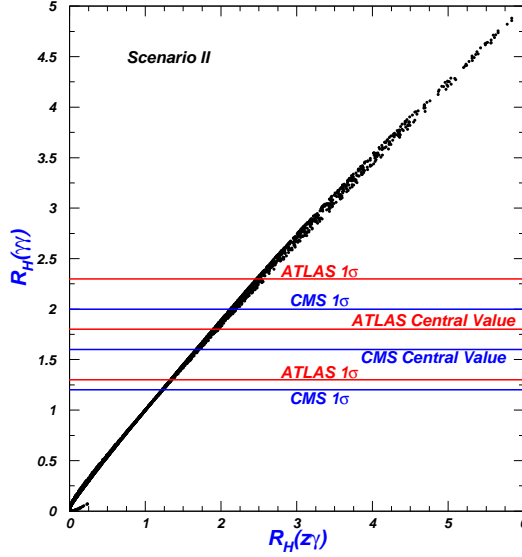


FIG. 6: Same as Fig. 3, but for  $R_H(\gamma\gamma)$  versus  $R_H(Z\gamma)$ .

than 0.02 for  $80 \text{ GeV} \leq m_{H^\pm} \leq 100 \text{ GeV}$ . The corresponding cross section of  $e^+e^- \rightarrow Zh$  is below the upper limit presented by the LEP [18].

In Fig. 6, we plot  $R_H(\gamma\gamma)$  versus  $R_H(Z\gamma)$ . We find that the two rates are also positively correlated for the scenario II. The  $1 \sigma$  range of diphoton experimental data will imply that  $R_H(Z\gamma)$  should be in the range of 1.2 and 2.5.

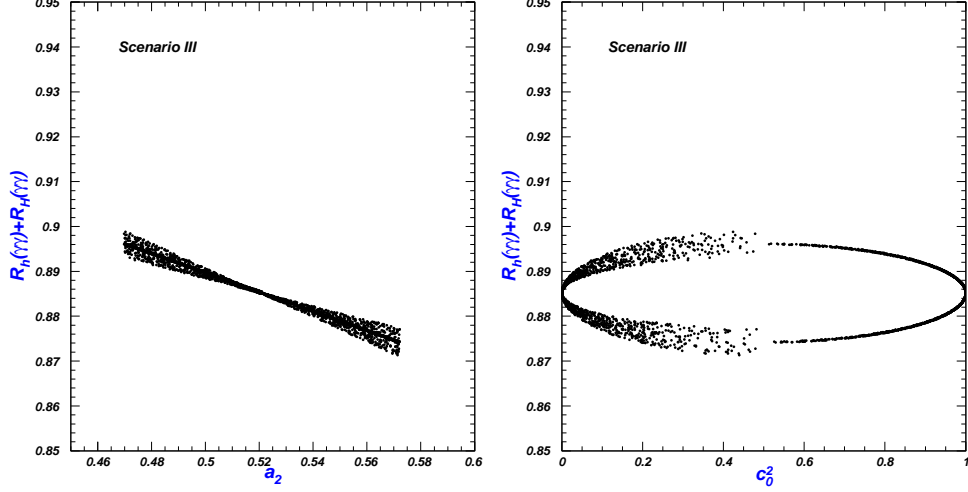


FIG. 7: The scatter plots of the parameter space projected on the planes of  $R_h(\gamma\gamma) + R_H(\gamma\gamma)$  versus  $a_2$  and  $c_0^2$ , respectively.

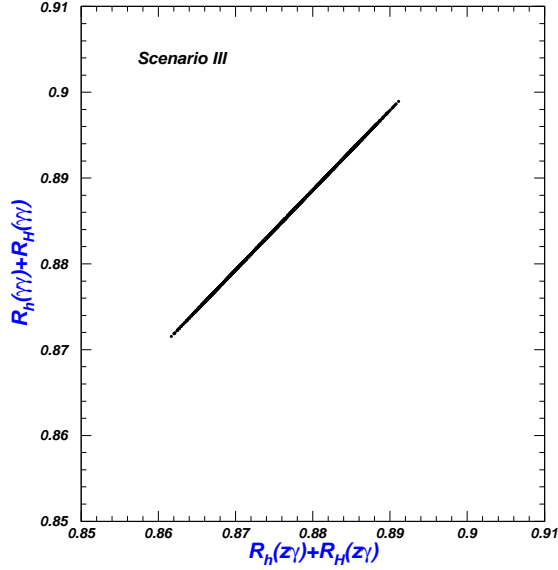


FIG. 8: Same as Fig. 3, but for  $R_h(\gamma\gamma) + R_H(\gamma\gamma)$  versus  $R_h(Z\gamma) + R_H(Z\gamma)$ .

### C. Scenario III

For the scenario III, the observed signal is from the almost degenerate  $h$  and  $H$ . We assume that the mass splitting of  $h$  and  $H$  is small enough not to be resolved at current statistics, but large enough so that there is hardly interference between the amplitudes of  $h$  and  $H$ ,  $|m_H - m_h| \gg \Gamma(h), \Gamma(H)$  [19]. Therefore, according to Eq. (10), both the absolute values of  $A - C$  and  $B$  must be very small, but not to equal to zero exactly. For this case, we can obtain a relation of  $m_{H^\pm} \simeq m_h \simeq m_H$  according to Eqs. (4), (7) and (10).

In Fig. 7, we plot  $R_h(\gamma\gamma)+R_H(\gamma\gamma)$  versus  $a_2$  and  $c_0^2$ , respectively. We find that the Higgs diphoton rate is suppressed compared to SM value,  $0.87 < R_h(\gamma\gamma)+R_H(\gamma\gamma) < 0.9$ , which is disfavored by the enhancement of diphoton data. Due to  $a_1 > 0$ ,  $a_2$  must be larger than zero to obtain a very small  $|B|$  ( $B = -a_1 v_d/2 + a_2 v_d v_t$ ). Thus,  $R_h(\gamma\gamma)+R_H(\gamma\gamma)$  is smaller than 1.0 since the  $H^\pm$  contributions will interfere destructively with the  $W$  contributions for  $a_2 > 0$ . The right panel shows that the large mixing angle  $\theta_0$  may appear. The reason is that  $|A - C|$  still may be smaller than  $|B|$  although  $|B|$  is very small.

In Fig. 8, we plot  $R_h(\gamma\gamma) + R_H(\gamma\gamma)$  versus  $R_h(Z\gamma) + R_H(Z\gamma)$ . We find that the two rates are also positively correlated and approximately equal.

#### IV. CONCLUSION

In the Higgs triplet model with  $Y=0$ , we study the Higgs boson  $\gamma\gamma$  and  $Z\gamma$  rates at the LHC. We obtained the following observations: (i) For the observed boson is the light Higgs  $h$ , whose diphoton rate can be within the  $1\sigma$  lower range of the ATLAS and CMS data. The heavy Higgs  $H$  production rate can be suppressed enough not to be observed at the LHC. (ii) For the observed Higgs is the heavy Higgs  $H$ , whose diphoton rate can be within the whole  $1\sigma$  range of the ATLAS and CMS data. The light Higgs  $h$  production rate can be suppressed enough not to be observed at the LEP. (iii) For the observed signal is from the almost degenerate  $h$  and  $H$ , the Higgs diphoton rate is suppressed compared to SM, which is disfavored the ATLAS and CMS data. (iv) The  $Z\gamma$  and  $\gamma\gamma$  rates are positively correlated for the above three scenarios.

#### Acknowledgment

This work was supported by the National Natural Science Foundation of China (NNSFC) under grant Nos. 11105116, 11005089, and 11175151.

## Appendix A: The expressions for $\Gamma(h \rightarrow \gamma\gamma)$ and $\Gamma(h \rightarrow Z\gamma)$

The charged fermion ( $f$ ), gauge boson ( $W$ ) and scalar ( $s$ ) can contribute to the decay widths of  $h \rightarrow \gamma\gamma$  and  $h \rightarrow Z\gamma$ , which are given by [12, 20]

$$\Gamma(h \rightarrow \gamma\gamma) = \frac{\alpha^2 m_h^3}{256\pi^3 v^2} \left| \sum_f N_f^c Q_f^2 y_f A_{1/2}^{\gamma\gamma}(\tau_f) + y_W A_1^{\gamma\gamma}(\tau_W) + Q_s^2 \frac{v\mu_{hss^*}}{2m_s^2} A_0^{\gamma\gamma}(\tau_s) \right|^2, \quad (\text{A1})$$

$$\begin{aligned} \Gamma(h \rightarrow Z\gamma) = & \frac{\alpha^2 m_h^3}{128\pi^3 s_W^2 c_W^2 v^2} (1 - m_Z^2/m_h^2)^3 \left| N_f^c Q_f y_f \frac{(Q_R^Z + Q_L^Z)}{2} A_{1/2}^{Z\gamma}(\tau_f, \lambda_f) \right. \\ & \left. + Q_W Q_W^Z y_W A_1^{Z\gamma}(\tau_W, \lambda_W) + Q_s Q_s^Z \frac{v g_{hss}}{2m_s^2} A_0^{Z\gamma}(\tau_s, \lambda_s) \right|^2, \end{aligned} \quad (\text{A2})$$

where  $\tau_i = m_h^2/4m_i^2$ ,  $\lambda_i = m_Z^2/4m_i^2$ ,  $Q_W = 1$ ,  $Q_W^Z = c_W^2$ .  $Q_{f,s}$  are the electric charges of fermion and scalar.  $N_f^c$  is the color factor for fermion  $f$ .  $Q_{R,L(s)}^Z = I_{R,L(s)}^3 - Q_{f(s)} s_W^2$  with  $I_{R,L(s)}^3$  being the third isospin components of chiral fermions (scalar).  $y_f$  and  $y_W$  denote the Higgs couplings to  $f\bar{f}$  and  $WW$  normalized to the corresponding SM values.  $g_{hss}$  is the coupling constant of  $hss$ . The loop functions  $A_{(0,1/2,1)}^{\gamma\gamma}$  and  $A_{(0,1/2,1)}^{Z\gamma}$  in Eqs. (A1) and (A2) are defined as

$$\begin{aligned} A_0^{\gamma\gamma}(\tau) &= -[\tau - f(\tau)]\tau^{-2}, \quad A_{1/2}^{\gamma\gamma}(\tau) = 2[\tau + (\tau - 1)f(\tau)]\tau^{-2}, \\ A_1^{\gamma\gamma}(\tau) &= -[2\tau^2 + 3\tau + 3(2\tau - 1)f(\tau)]\tau^{-2}, \\ A_0^{Z\gamma}(\tau, \lambda) &= I_1(\tau, \lambda), \quad A_{1/2}^{Z\gamma}(\tau, \lambda) = -2[I_1(\tau, \lambda) - I_2(\tau, \lambda)], \\ A_1^{Z\gamma}(\tau, \lambda) &= [2(1 + 2\tau)(1 - \lambda) + (1 - 2\tau)]I_1(\tau, \lambda) - 8(1 - \lambda)I_2(\tau, \lambda), \end{aligned} \quad (\text{A3})$$

where

$$\begin{aligned} I_1(\tau, \lambda) &= -\frac{1}{(\tau - \lambda)} + \frac{1}{(\tau - \lambda)^2} [f(\tau) - f(\lambda)] + \frac{2\lambda}{(\tau - \lambda)^2} [g(\tau) - g(\lambda)], \\ I_2(\tau, \lambda) &= \frac{1}{(\tau - \lambda)} [f(\tau) - f(\lambda)], \end{aligned} \quad (\text{A4})$$

with the functions  $f(\tau)$  and  $g(\tau)$  given by

$$f(\tau) = \begin{cases} (\sin^{-1} \sqrt{\tau})^2, & \tau \leq 1 \\ -\frac{1}{4} [\log \frac{1+\sqrt{1-\tau^{-1}}}{1-\sqrt{1-\tau^{-1}}} - i\pi]^2, & \tau > 1 \end{cases}, \quad g(\tau) = \begin{cases} \sqrt{\tau^{-1}-1}(\sin^{-1} \sqrt{\tau}), & \tau \leq 1 \\ \frac{\sqrt{1-\tau^{-1}}}{2} [\log \frac{1+\sqrt{1-\tau^{-1}}}{1-\sqrt{1-\tau^{-1}}} - i\pi], & \tau > 1. \end{cases} \quad (\text{A5})$$

---

[1] S. Chatrchyan et al. [CMS Collaboration], Phys. Lett. B **716**, 30 (2012).

- [2] G. Aad et al. [ATLAS Collaboration], Phys. Lett. B **716**, 1 (2012).
- [3] The TEVNPH Working Group for the CDF and D0 Collaborations, arXiv:1207.0449.
- [4] See, e.g., U. Ellwanger, C. Hugonie, Adv. High Energy Phys. **2012**, 625389 (2012); K. Hagiwara, J. S. Lee, J. Nakamura, JHEP **1210**, 002 (2012); N. Christensen, T. Han, S. Su, Phys. Rev. D **85**, 115018 (2012); B. Kyae, J.-C. Park, arXiv:1207.3126; J. Cao *et al.*, JHEP **1210**, 079 (2012); JHEP **1203**, 086 (2012); Phys. Lett. B **710**, 665 (2012); H. An, T. Liu, L.-T. Wang, Phys. Rev. D **86**, 075030 (2012); M. Berg, I. Buchberger, D. M. Ghilencea, C. Petersson, arXiv:1212.5009; K. Cheung, C.-T. Lu, T.-C. Yuan, arXiv:1212.1288; T. Liu, L. Wang, J. M. Yang, arXiv:1301.5479; M. Carena, S. Gori, I. Low, N. R. Shah, C. E. M. Wagner, JHEP **1302**, 114 (2013); E. J. Chun, P. Sharma, arXiv:1301.1437; T. Kitahara, T. Yoshinaga, arXiv:1303.0461; Z. Kang, Y. Liu, G. Ning, arXiv:1301.2204; J. Ke, M.-X. Luo, L.-Y. Shan, K. Wang, L. Wang, Phys. Lett. B **718**, 1334 (2013); T. Li, J. A. Maxin, D. V. Nanopoulos, J. W. Walker, Eur. Phys. Jour. C **72**, 2246 (2012); W.-Z. Feng, P. Nath, arXiv:1303.0289; A. Delgado, G. Nardini, M. Quiros, arXiv:1303.0800.
- [5] L. Wang, J. M. Yang, Phys. Rev. D **84**, 075024 (2011); Phys. Rev. D **79**, 055013 (2009); T. Han, H. E. Logan, B. McElrath, L.-T. Wang, Phys. Lett. B **563**, 191 (2003); C. R. Chen, K. Tobe, C. P. Yuan, Phys. Lett. B **640**, 263 (2006); J. Reuter, M. Tonini, JHEP **1302**, 077 (2013); X.-F. Han, L. Wang, J. M. Yang, J. Zhu, Phys. Rev. D **87**, 055004 (2013).
- [6] See, e.g., C. Haluch, R. Matheus, Phys. Rev. D **85**, 095016 (2012); X.-G. He, B. Ren, J. Tandean, Phys. Rev. D **85**, 093019 (2012); A. Arhrib, R. Benbrik, C.-H. Chen, arXiv:1205.5536; L. Wang, X.-F. Han, JHEP **1205**, 088 (2012); S. Chang *et al.*, arXiv:1210.3439; N. Chen, H.-J. He, JHEP **1204**, 062 (2012); T. Abe, N. Chen, H.-J. He, JHEP **1301**, 082 (2013); C. Han *et al.*, arXiv:1212.6728; C.-W. Chiang, K. Yagyu, arXiv:1303.0168; R. Jora, S. Nasri, J. Schechter, arXiv:1302.6344; A. Celis, V. Ilisie, A. Pich, arXiv:1302.4022.
- [7] A. G. Akeroyd, S. Moretti, Phys. Rev. D **86**, 035015 (2012); A. Arhrib *et al.*, JHEP **1204**, 136 (2012); L. Wang, X.-F. Han, Phys. Rev. D **86**, 095007 (2012); Phys. Rev. D **87**, 015015 (2013); Y. Kajiyama, H. Okada, K. Yagyu, arXiv:1303.3463; P. S. B. Dev, D. K. Ghosh, N. Okada, I. Saha, arXiv:1301.3453; F. Arbabifar, S. Bahrami, M. Frank, Phys. Rev. D **87**, 015020 (2013); C. Englert, E. Re, M. Spannowsky, arXiv:1302.6505.
- [8] Y. Cai, W. Chao, S. Yang, JHEP **1212**, 043 (2012).

- [9] J. Cao, P. Wan, J. M. Yang, J. Zhu, arXiv:1303.2426.
- [10] D. A. Ross, M. J. G. Veltman, Nucl. Phys. B **95**, 135 (1975); J. F. Gunion, R. Vega and J. Wudka, Phys. Rev. D **42**, 1673 (1990).
- [11] C. Chiang and K. Yagyu, arXiv:1207.1065; P. S. B. Dev et al., arXiv:1301.3453; B. Coleppa, K. Kumar, H. E. Logan, Phys. Rev. D **86**, 075022 (2012); J. Cao, L. Wu, P. Wu, J. M. Yang, arXiv:1301.4641.
- [12] C.-S. Chen, C.-Q. Geng, D. Huang, L.-H. Tsai, arXiv:1302.0502; arXiv:1301.4694.
- [13] P. F. Perez, H. H. Patel, M. J. Ramsey-Musolf, K. Wang, Phys. Rev. D **79**, 055024 (2009).
- [14] S. Kanemura, K. Yagyu, Phys. Rev. D **85**, 115009 (2012).
- [15] ALEPH Collaboration, Phys. Lett. B **543**, 1 (2002); J. Abdallah, et al. [ DELPHI Collaboration], Eur. Phys. Jour. C **34**, 399 (2004).
- [16] A. Djouadj, J. Kalinowski, and M. Spira, Comput. Phys. Commun. **108**, 56 (1998).
- [17] [CMS Collaboration], CMS-PAS-HIG-12-049.
- [18] R. Barate et al. [LEP Working Group for Higgs boson searches and ALEPH and DELPHI and L3 and OPAL Collaborations], Phys. Lett. B **565**, 61 (2003); S. Schael et al. [ALEPH and DELPHI and L3 and OPAL and LEP Working Group for Higgs Boson Searches Collaborations], Eur. Phys. Jour. C **47**, 547 (2006).
- [19] B. Batell, D. McKeen, and M. Pospelov, JHEP **1210**, 104 (2012).
- [20] A. Djouadi, Phys. Rept. **459**, 1 (2008).